Thermochimica Acta 499 (2010) 155–159

Contents lists available at ScienceDirect

Thermochimica Acta

journal homepage: www.elsevier.com/locate/tca

Crystal structure and thermodynamic properties of potassium antimony tungsten oxide

Aleksandr V. Knyazev[a,*], Ivan G. Tananaev[b], Nataliya Yu. Kuznetsova[a], Nataliya N. Smirnova[a], Irene A. Letyanina[a], Igor V. Ladenkov[a]

[a] Nizhny Novgorod State University, Gagarin Prospekt 23/2, Nizhny Novgorod, 603950, Russia
[b] Institute of Physical Chemistry and Electrochemistry, Russian Academy of Sciences, 31 Leninsky prospect, Moscow GSP-1, 119991, Russia

ARTICLE INFO

Article history:
Received 17 September 2009
Received in revised form
24 November 2009
Accepted 1 December 2009
Available online 6 December 2009

Keywords:
Pyrochlore
Heat capacity
Thermodynamic functions
X-ray diffraction
Potassium antimony tungsten oxide

ABSTRACT

In the present work potassium antimony tungsten oxide with pyrochlore structure is refined by the Rietveld method (space group *Fd*3*m*, *Z* = 8). The temperature dependences of heat capacity have been measured for the first time in the range from 7 to 370 K for this compound. The experimental data were used to calculate standard thermodynamic functions, namely the heat capacity $C_p^\circ(T)$, enthalpy $H^\circ(T) - H^\circ(0)$, entropy $S^\circ(T) - S^\circ(0)$ and Gibbs function $G^\circ(T) - H^\circ(0)$, for the range from $T \rightarrow 0$ to 370 K. The differential scanning calorimetry was applied to measure the incongruent melting temperature of compound under study. The high-temperature X-ray diffraction was used for the determining thermal expansion coefficients.

1. Introduction

The mixed oxides of stoichiometry $A_2B_2O_7$ and $A_2B_2O_6$ with the pyrochlore structure (space group *Fd*3*m*) attract attention of scientists as a result of their interesting structural aspects and their wide applications. The technological applications of these materials are chiefly derived from their magnetic properties, in catalysis, and their growing use in the field of electronics [1–3].

The object of our investigation is complex oxide containing antimony, tungsten and potassium. In order to understand the relations among structure and energetic in a fundamental sense, and to correlate reactivity at high temperature and materials compatibility in applications, thermodynamic data are essential. Despite the extensive interest in defect pyrochlores, there is no any thermodynamic data and other physicochemical data are presented in bare number of publications. Therefore detailed investigations of these compounds are especially important.

The goals of this work include detailed structural investigation, studies of thermal stability, calorimetric determination of the temperature dependence of the heat capacity $C_p^\circ = f(T)$ of $KSbWO_6$ from 7 to 370 K, detection of the possible phase transitions, and calculation of the standard thermodynamic functions $C_p^\circ(T)$, $H^\circ(T) - H^\circ(0)$, $S^\circ(T) - S^\circ(0)$ and $G^\circ(T) - H^\circ(0)$ in the range from $T \rightarrow 0$ to 370 K.

2. Experimental

2.1. Sample

Sample of $KSbWO_6$ was prepared by the solid-state reaction between tungsten oxide, antimony(III) oxide and potassium nitrate. The synthesis was performed in a porcelain crucible, into which the reaction mixture with the atomic ration 1K + 1W + 1Sb was loaded. The mixture was calcined from 673 to 1073 K with temperature rise on 200 K and holding reaction mixture at every temperature during 3 h to prevent sublimation of components. Then the mixture was calcined at 1073 K for 20 h, undergoing regrinding every 5 h to increase crystallinity. To prove the atomic ration 1K + 1W + 1Sb the obtained sample was analyzed on a Shimadzu energo-dispersive roentgen fluorescent spectrometer EDX-900HS (from $_{11}$Na to $_{92}$U) with sensitive detector without liquid nitrogen.

For structural investigations, an X-ray diffraction pattern of a $KSbWO_6$ sample was recorded on a Shimadzu X-ray diffractometer XRD-6000 (Cu Kα radiation, geometry θ–2θ) in the 2θ range from 10° to 120° with scan increment of 0.02°. Rietveld analysis and structure refinement [4] were carried out using RIETAN-94 software [5]. The X-ray data and estimated impurity content (0.5–1 wt.%) in the substances led us to conclude that the

* Corresponding author. Tel.: +7 831 465 62 06; fax: +7 831 434 50 56.
E-mail address: knav@uic.nnov.ru (A.V. Knyazev).

0040-6031/$ – see front matter © 2009 Elsevier B.V. All rights reserved.
doi:10.1016/j.tca.2009.12.002

Table 1
Details of the X-ray diffraction experiment and the results of the structure refinement for $KSbWO_6$.

Space group	*Fd*3*m*
Z	8
2θ range,°	10–120
a, Å	10.23671(7)
V, Å^3	1072.71(1)
Number of reflections	63
Number of refined parameters:	27
Structural parameters	6
Others	21
R_{wp}; R_p, %	3.75; 2.63
$R_{wp} = \{(\Sigma w_i[y_{iobs} - y_{icalc}]^2/(\Sigma w_i[y_{iobs}]^2)\}^{1/2}$; $R_p = (\Sigma\lvert y_{iobs} - y_{icalc}\rvert)/(\Sigma y_{iobs})$.	

studied sample was an individual crystalline compound. The high-temperature X-ray diffraction was carried out on a Shimadzu X-ray diffractometer XRD-6000 using Sample Heating Attachment HA-1001.

2.2. Apparatus and measurement procedure

To measure the heat capacity C_p° of the tested substance in the range from 7 to 370 K a BKT-3.0 automatic precision adiabatic vacuum calorimeter with discrete heating was used. The calorimeter design and the operation procedure were described earlier [6,7]. The calorimeter was tested by measuring the heat capacity of high-purity copper and reference samples of synthetic corundum and K-2 benzoic acid. The analysis of the results showed that measurement error of the heat capacity of the substance at helium temperature was within ±2% (5 < *T* < 20 K), then it decreased to ±0.5% as the temperature was rising to 40 K, and was equal to ±0.2% at *T* > 40 K. Temperatures of phase transitions can be determined with the error of ±0.02 K.Thermal behavior was carried out with DSC Labsys from Setaram in a platinum crucible ranging from 298 to 1420 K (heating rate 0.167 K/s).

3. Results and discussion

3.1. Crystal structure

The structure of $KSbWO_6$ was refined assuming space group *Fd*3*m*. The initial model included the atomic coordinates in the structure of $KNbWO_6$ [8]. The details of the X-ray diffraction experiment and structure refinement data are listed in Table 1.

Fig. 1 represents the measured, simulated, and difference X-ray diffraction patterns for $KSbWO_6$, as well as a pattern of lines

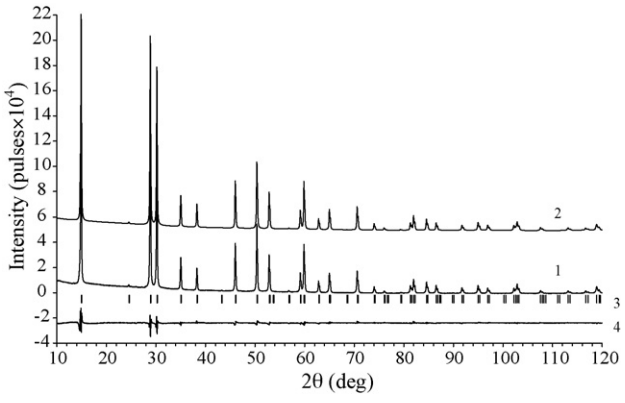

Fig. 1. Fragments of (1) observed, (2) simulated, and (4) difference X-ray diffraction patterns for $KSbWO_6$, (3) Bragg reflections. The simulated pattern is shifted relative to the observed pattern.

Table 2
Coordinates and isotropic thermal parameters of atoms in the structure of $KSbWO_6$.

Atom	Site	*x*	*y*	*z*	Occ	*B* (Å^2)
K	32e	0.4010(5)	0.4010(5)	0.4010(5)	0.25	2.0(3)
Sb	16c	0	0	0	0.5	0.85(2)
W	16c	0	0	0	0.5	0.85(2)
O	48f	0.3206(3)	0.125	0.125		0.9(1)

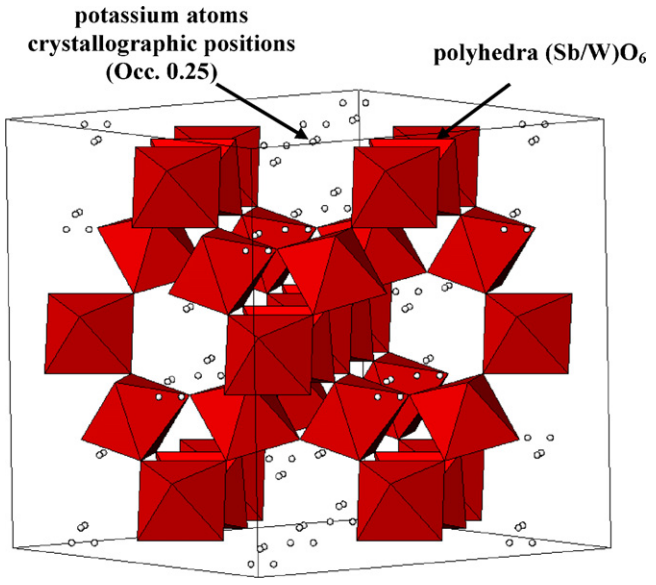

Fig. 2. Fragment of $KSbWO_6$ structure.

corresponding to reflection maxima. There is a good agreement between the measured and simulated patterns. Table 2 lists the coordinates of the atoms and their isotropic thermal parameters. The refined model yielded positive isotropic thermal parameters *B* for all atoms. The Sb/W–O bond lengths are 1.949 ± 0.001 Å, and K–O bond lengths are 2.874 ± 0.005 Å and 3.346 ± 0.005 Å (Table 3).

Fig. 2 represents a fragment of the $KSbWO_6$ structure. The $(Sb/W)O_6$ octahedra share corners to form a three-dimensional framework possessing tunnels running down the *c*-axis in which the potassium cations are located. The Sb/W cation is located in the 16c Wyckoff position (0, 0, 0) and the oxygen is in 48f sites (*x*, 1/8, 1/8). The location of the potassium is in the 32e site (*x*, *x*, *x*) (Table 2).

3.2. Heat capacity

The C_p° measurements were carried out between 7 and 370 K. The mass of the sample loaded in the calorimetric ampoule of the BKT-3.0 calorimeter was 1.4196 g. There was obtained 191 experimental C_p° values in two series of experiments. The heat capacity of the sample varied from 30% to 70% of the total heat capacity of calorimetric ampoule + substance over the range between 7 and 370 K. The experimental points of C_p° in the temperature interval between *T* = (7 and 370) K were fitted by means of the least-squares method and polynomial equations (Eqs. (1) and (2)) of the C_p° vs. temperature have been obtained. The corresponding coefficients

Table 3
Interatomic distances and valence angles in the structure of $KSbWO_6$.

Bond	*d* (Å)	Angle	ω (°)
Sb/W–O (6×)	1.949(1)	O–Sb/W–O (3×)	86.8
K–O (3×)	2.874(5)	O–Sb/W–O (3×)	93.2
K–O (3×)	3.346(5)		

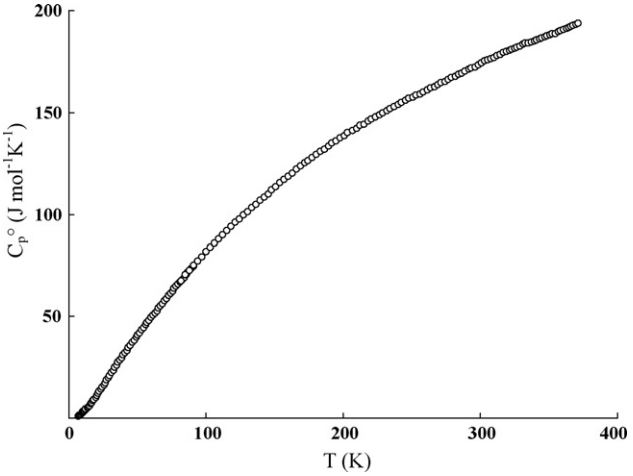

Fig. 3. Temperature dependences of heat capacity of $KSbWO_6$.

(A, B, C, etc.) are given in Table S2.

$$C_p^\circ(T) = A + B\cdot\left(\frac{T}{30}\right) + C\cdot\left(\frac{T}{30}\right)^2 + D\cdot\left(\frac{T}{30}\right)^3 + E\cdot\left(\frac{T}{30}\right)^4 + F\cdot\left(\frac{T}{30}\right)^5 + G\cdot\left(\frac{T}{30}\right)^6 + H\cdot\left(\frac{T}{30}\right)^7 + I\cdot\left(\frac{T}{30}\right)^8 + J\cdot\left(\frac{T}{30}\right)^9 \quad (1)$$

$$\ln C_p^\circ(T) = A + B\cdot\ln\left(\frac{T}{30}\right) + C\cdot\left\{\ln\left(\frac{T}{30}\right)\right\}^2 + D\cdot\left\{\ln\left(\frac{T}{30}\right)\right\}^3 + E\cdot\left\{\ln\left(\frac{T}{30}\right)\right\}^4 + F\cdot\left\{\ln\left(\frac{T}{30}\right)\right\}^5 + G\cdot\left\{\ln\left(\frac{T}{30}\right)\right\}^6 + H\cdot\left\{\ln\left(\frac{T}{30}\right)\right\}^7 + I\cdot\left\{\ln\left(\frac{T}{30}\right)\right\}^8 + J\cdot\left\{\ln\left(\frac{T}{30}\right)\right\}^9 \quad (2)$$

Their root mean square deviation from the averaging $C_p^\circ = f(T)$ curve was ±0.15% in the range T = (6–30) K, ±0.075% from T = (25–150) K, ±0.15% between T = (130 and 370) K.

The experimental values of the molar heat capacity of $KSbWO_6$ over the range from 7 to 370 K and the averaging $C_p^\circ = f(T)$ plot are presented in Fig. 3 and Table S1. The heat capacity C_p° of this substance gradually increases with rising temperature and does not show any peculiarities until 370 K.

3.3. Standard thermodynamic functions

To calculate the standard thermodynamic functions (Table 4) of potassium antimony tungsten oxide, its C_p° values were extrapolated from the starting temperature of the measurement beginning at approximately 7–0 K by Debye's function of heat capacity:

$$C_p^\circ = nD\left(\frac{\theta_D}{T}\right), \quad (3)$$

where D is the symbol of Debye's function, n = 3 and $\theta_D(KSbWO_6)$ = 87.5 K are specially selected parameters. Eq. (3) with the above parameters describes the experimental C_p° values of the compound between 7 and 13 K with the error of ±1.67%.

In calculating the functions it was assumed that Eq. (3) reproduces the C_p° values of $KSbWO_6$ at T < 7 K with the same error. The calculations of $H^\circ(T) - H^\circ(0)$ and $S^\circ(T) - S^\circ(0)$ were made by the numerical integration of $C_p^\circ = f(T)$ and $C_p^\circ = f(\ln T)$ curves, respectively, and the Gibbs function $G^\circ(T) - H^\circ(0)$ was estimated from the enthalpies and entropies at the corresponding temperatures [9]. It was suggested that the error of the function values was ±1% at T < 40 K, ±0.5% between 40 and 80 K, ±0.2% in the range from 80 to 350 K.

The absolute entropies of $KSbWO_6$ (Table 4) and the corresponding simple substances W (cr), Sb (cr), K (cr) [10] and O_2 (g) [11] were used to calculate the standard entropy of formation of the compound under study at 298.15 K, $\Delta_f S^\circ$(298.15, $KSbWO_6$, cr) = −552.6 ± 1.7 J K^{-1} mol^{-1}.

In order to correlate obtained thermodynamic and structural data it is important to apply to the fractal version of Debye's theory. The values of the fractal dimension D – the most significant parameter of the fractal version of Debye's theory of heat capacity of solids [12,13] – were determined from the experimental data on the heat capacity of compounds under investigation. The values of D were estimated using the technique described in works [14,15]

Table 4
Thermodynamic functions of crystalline $KSbWO_6$; M($KSbWO_6$) = 440.6947 g mol^{-1}, p° = 0.1 MPa.

T (K)	$C_p^\circ(T)$ (J K^{-1} mol^{-1})	$H^\circ(T) - H^\circ(0)$ (kJ mol^{-1})	$S^\circ(T)$ (J K^{-1} mol^{-1})	$-[G^\circ(T) - H^\circ(0)]$ (kJ mol^{-1})
0	0	0	0	0
5	0.3625	0.0005	0.1208	0.000151
10	2.726	0.0072	0.9538	0.002369
15	6.395	0.0298	2.743	0.01134
20	10.83	0.0725	5.164	0.03083
25	15.96	0.1393	8.123	0.06377
30	21.26	0.2323	11.50	0.1128
35	26.50	0.3518	15.18	0.1794
40	31.29	0.4965	19.03	0.2649
45	36.00	0.6647	22.99	0.3699
50	40.69	0.8565	27.03	0.4950
60	49.51	1.308	35.24	0.8062
70	57.93	1.845	43.50	1.200
80	66.30	2.467	51.79	1.676
90	74.51	3.172	60.09	2.236
100	81.69	3.953	68.31	2.878
110	88.71	4.805	76.43	3.602
120	95.28	5.726	84.43	4.406
130	101.4	6.709	92.30	5.290
140	107.3	7.753	100.0	6.252
150	113.0	8.854	107.6	7.290
160	118.7	10.01	115.1	8.404
170	124.2	11.23	122.5	9.592
180	129.4	12.50	129.7	10.85
190	134.1	13.81	136.8	12.19
200	138.4	15.18	143.8	13.59
210	142.5	16.58	150.7	15.06
220	146.5	18.03	157.4	16.60
230	150.2	19.51	164.0	18.21
240	154.0	21.03	170.5	19.88
250	157.5	22.59	176.8	21.62
260	160.7	24.18	183.1	23.42
270	163.9	25.80	189.2	25.28
273.15	165.0	26.32	191.1	25.88
280	167.2	27.46	195.2	27.20
290	170.6	29.15	201.1	29.18
298.15	173.4	30.55	205.9	30.84
300	174.1	30.87	207.0	31.22
310	177.4	32.63	212.8	33.32
320	180.4	34.42	218.4	35.48
330	183.1	36.24	224.0	37.69
340	185.5	38.08	229.5	39.96
350	187.9	39.95	234.9	42.28
360	190.6	41.84	240.3	44.66
370	193.4	43.76	245.5	47.09

Table 5
Structural and thermodynamic parameters of compounds with common formula $M^IA^VWO_6$ [18–20].

$M^IA^VWO_6$	$r(M^I)$ CN = VI (Å)	Distance (M^I–O) (Å)	T_{dec} (K)	Δ_fS° (298.15 K) ($J\,K^{-1}\,mol^{-1}$)	$\Delta_{f\text{-}ox}S^\circ$(298.15 K) ($J\,K^{-1}\,mol^{-1}$)	$\Delta(\nu c_p)$, (298.15 K) ($J\,K^{-1}\,mol^{-1}$)
$LiVWO_6$	0.76	1.995(9) (2×) 2.467(8) (4×)	1022	−532.1 ± 1.6	14.1	1.2
$NaVWO_6$	1.02	2.343(8) (2×) 2.403(6) (4×)	1031	−543.6 ± 1.6	6.1	−2.0
$KSbWO_6$	1.38	2.874(5) (3×) 3.346(5) (3×)	1361	−552.6 ± 1.7	19.3	4.8
$RbNbWO_6$	1.52	3.250(6×)	1465	−538.5 ± 1.6	15.6	4.5
$CsTaWO_6$	1.67	3.186(4) (6×)	1588	−553.2 ± 1.7	0.9	−3.9

with the use of Eq. (4):

$$C_v = 3D(D+1)kN\gamma(D+1)\xi(D+1)\left(\frac{T}{\theta_{max}}\right)^D, \quad (4)$$

where N is the number of atoms in a formula unit, k the Boltzmann constant, $\gamma(D+1)$ the γ-function, $\xi(D+1)$ the Riemann ξ-function, and θ_{max} is the characteristic temperature. According to Ref. [16], $D=1$ corresponds to the solids with chain structure, $D=2$ to those with a layered structure, and $D=3$ [17] to those with a spatial structure. For the tested compound $D=3$ at $T>30$ K correspond to the frame structure, that good coordinates with our X-ray diffraction data.

For the purpose of analyzing chemical thermodynamics data of triple oxides containing tungsten with common formula $M^IA^VWO_6$ we calculated entropies of formation from the oxides [10,11] for five compounds under study [18–20] (Eqs. (5) and (6), Table 5).

$$0.5\cdot M^I_2O(s) + 0.5\cdot A^V_2O_5(s) + WO_3(s) = M^IA^VWO_6(s) \quad (5)$$

$$\Delta_{f\text{-}ox}S^\circ(298.15) = S^\circ(M^IA^VWO_6,\ s,\ 298.15) - 0.5\cdot S^\circ(M^I_2O,\ s,\ 298.15) - 0.5\cdot S^\circ(A^V_2O_5,\ s,\ 298.15) - S^\circ(WO_3,\ s,\ 298.15) \quad (6)$$

Our studies show that $\Delta_{f\text{-}ox}S^\circ$ values depend on structural type and structural peculiarities' of compounds. The represented compounds crystallize in two structural types: brannerite ($LiVWO_6$ $NaVWO_6$) and defect pyrochlore ($KSbWO_6$, $RbNbWO_6$, $CsTaWO_6$). Therefore it is reasonable to analyze thermodynamic data within the bounds of each structural type. However, we could observe common tendency to decreasing entropies of formation from the oxides with increasing degree of atomic packing in the structure. Cations have octahedral environment in all compounds under study, but bond distances in alkali metal coordination polyhedra are the most variable in the network of each structural type. For example, in $LiVWO_6$ there is a big distortion LiO_6-octahedra due to unusual coordination for lithium. This leads to greater value of $\Delta_{f\text{-}ox}S^\circ$ in comparison with sodium counterpart. For pyrochlores bond distance M^I–O (see Table 5) decreases in row $KSbWO_6$–$RbNbWO_6$–$CsTaWO_6$ in spite of increasing alkali metal ionic radius, last fact leads to more close-packed structure and small values $\Delta_{f\text{-}ox}S^\circ$. It is interesting to notice that there is the reverse tendency of decomposition temperatures change in comparison with entropies of formation from the oxides in studied compounds row.

Table 6
Parameters of unit cells and thermal expansion coefficients temperature for $KSbWO_6$.

T (K)	a (Å)	V (Å^3)	Density ($g\,cm^{-3}$)	$\alpha\times10^6$ (K^{-1})
298	10.23671(7)	1072.71(1)	5.46	2.47
373	10.2383(8)	1073.2(2)	5.45	2.92
473	10.2418(8)	1074.3(2)	5.45	3.52
573	10.2455(7)	1075.5(1)	5.44	4.12
673	10.2522(6)	1077.6(1)	5.43	4.72
773	10.2556(9)	1078.7(3)	5.43	5.31
873	10.2604(8)	1080.2(2)	5.42	5.91
973	10.2682(8)	1082.6(2)	5.41	6.50
1073	10.2743(9)	1084.6(3)	5.40	7.09
1173	10.2811(9)	1086.7(3)	5.39	7.69
1273	10.2916(8)	1090.1(2)	5.37	8.28

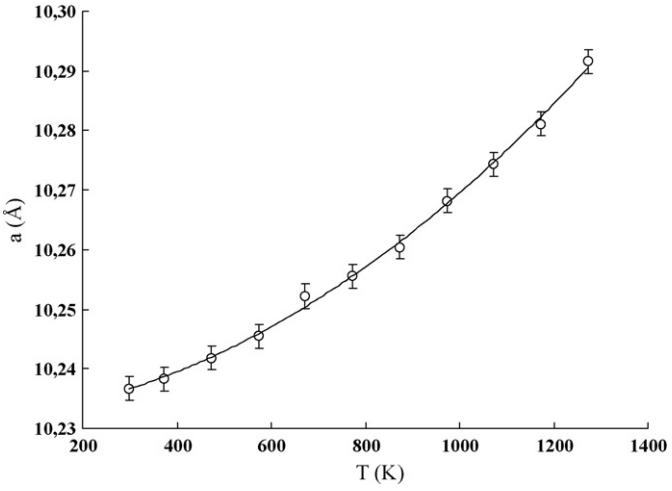

Fig. 4. Plot of unit cell parameter vs. temperature for $KSbWO_6$.

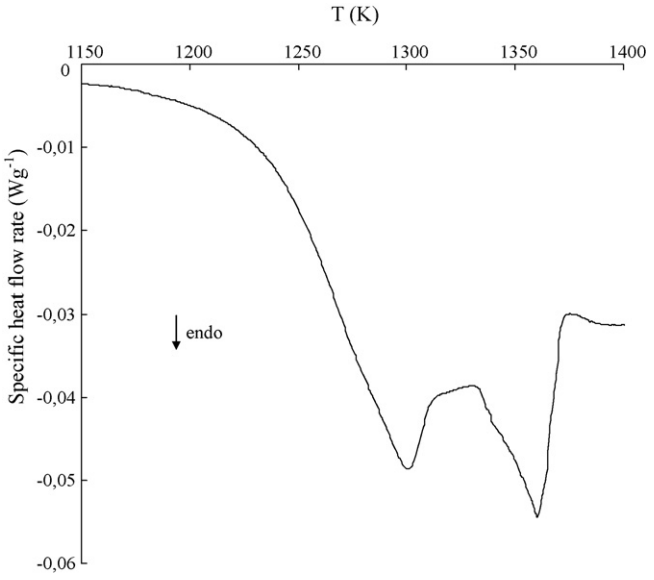

Fig. 5. Plot of the DTA-signal against temperature for $KSbWO_6$.

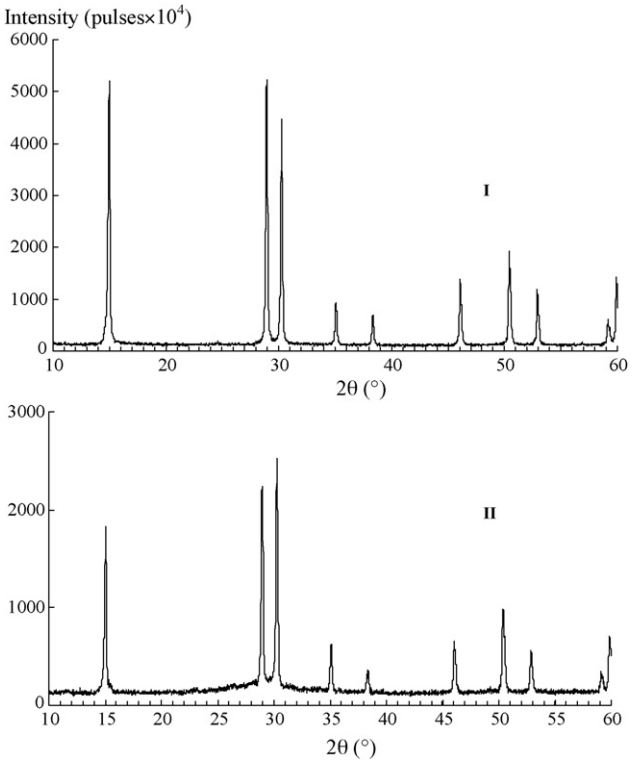

Fig. 6. X-ray diffraction patterns for $KSbWO_6$ (I) recorded at room temperature, (II) recorded at room temperature after heating up to 1315 K.

We would like to emphasize that the mean change of heat capacity in reactions of synthesis from oxides (5) for all compounds with common formula $M^IA^VWO_6$ is small enough and equal to $0.9\,J\,K^{-1}\,mol^{-1}$. Therefore in concordance with Kirchhoff law reaction (5) enthalpies do not depend on temperature and hereupon $\Delta_{f\text{-}ox}G^\circ$ is determined only entropy summand.

Thus represented analysis allows revealing some patterns of relationship in classical triad composition-structure-property.

3.4. High-temperature X-ray diffraction

The temperature dependence of the unit cell parameter is plotted in Fig. 4 and Table 6, and it is described by the following square polynomial:

$$a = 3.07 \times 10^{-8} \cdot T^2 + 7.01 \times 10^{-5} \cdot T + 10.2318 (298 \le T \le 1273\,K) \quad (5')$$

The average thermal expansion coefficient $\alpha_{av} = 5.32 \times 10^{-6}\,K^{-1}$ obtained for the potassium antimony tungsten oxide under investigation allows us to assign this pyrochlore to the class of medium-expansion compounds. The unit cell parameter a of this substance gradually increases with rising temperature and does not show any anomalies until 1273 K. This fact authenticates about lack of any transition at this temperature interval.

3.5. Differential scanning calorimetry

Joint application of the high-temperature X-ray diffraction and thermal analysis (TG–DTA) made it possible to establish some peculiarities of processes taking place in the compounds under investigation during heating. Fig. 5 represents DTA curves of $KSbWO_6$, where we can see two endothermic effects at 1302 and 1361 K. It was not observed any mass changes on TG curve during experiment, so we can draw a conclusion that the stoichiometric composition of system did not change. The first effect is connected with irreversible polymorphic transition cubicI ($a = 10.23671(7)$ Å) → cubicII ($a = 10.2338(9)$ Å) without change of crystal system, which can be confirmed by X-ray diffraction data. Fig. 6 represents two X-ray diffraction patterns: the first was recorded at room temperature, the second- at room temperature after heating up to 1315 K. As we can see from Fig. 6 there are significant changes of the first three peaks intensity concerning each other. The second effect is connected with incongruent melting. After the second effect parent phase was not detected. Melting products, found out by XRD analysis, were not identified due to complexity their compositions and lack in PDF 4 and FindIt XRD databases.

Appendix A. Supplementary data

Supplementary data associated with this article can be found, in the online version, at doi:10.1016/j.tca.2009.12.002.

References

[1] M.A. Subramanian, G. Aravamudan, G.V. Subba Rao, Progr. Solid State Chem. 15 (1983) 55.
[2] J.H.H. ter Maat, M.P. van Dijk, G. Roelofs, H. Bosch, G.M.H. van de Velde, P.J. Gellings, A.J. Burggraaf, Mater. Res. Bull. 19 (1984) 1271.
[3] J.B. Goodenough, R.N. Castellano, J. Solid State Chem. 44 (1982) 108.
[4] H.M. Rietveld, Acta Crystallogr. 22 (Part 1) (1967) 151.
[5] I.F. Rietveld, in: R.A. Young (Ed.), Analysis Programs RIETAN and PREMOS and Special Applications, The Rietveld Method, Oxford University Press, Oxford, 1993, p. 236.
[6] R.M. Varushchenko, A.I. Druzhinina, E.L. Sorkin, J. Chem. Thermodyn. 29 (1997) 623.
[7] V.M. Malyshev, G.A. Milner, E.L. Sorkin, V.F. Shibakin, Prib. Tekh. Eksp. 6 (1985) 195.
[8] D.W. Murphy, R.J. Cava, K. Rhyne, R.S. Roth, A. Santoro, S.M. Zahurak, J.L. Dye, Solid State Ionics 18 (1986) 799.
[9] B.V. Lebedev, Thermochim. Acta 297 (1997) 143.
[10] M.W. Jr., Chase, NIST-JANAF Thermochemical Tables, Fourth Edition, J. Phys. Chem. Ref. Data, Monograph 9, 1998, 1–1951.
[11] J.D. Cox, D.D. Wagman, V.A. Medvedev, Codata Key Values for Thermodynamics, New York, 1984.
[12] T.S. Yakubov, Dokl. Akad. Nauk SSSR 310 (1990) 145.
[13] A.D. Izotov, O.V. Shebershnyova, K.S. Gavrichev, Third All-union Conference on Thermal Analysis and Calorimetry, Kazan, 1996.
[14] B.V. Lebedev, A.V. Markin, V.A. Davydov, L.S. Kashevarova, A.V. Rakhmanina, Thermochim. Acta 399 (2003) 99.
[15] B.V. Lebedev, A.V. Markin, Phys. Solid State 44 (2002) 434.
[16] V.V. Tarasov, Zh. Obshch. Khim. 26 (1952) 1374.
[17] V.V. Tarasov, Problems of Glass Physics, Stroyizdat, Moscow, 1979.
[18] A.V. Knyazev, M. Mączka, N.N. Smirnova, L. Macalik, N.Yu. Kuznetsova, I.A. Letyanina, J. Solid State Chem. 182 (2009) 3003–3012.
[19] A.V. Knyazev, M. Maczka, N.Yu. Kuznetsova, J. Hanuza, A.V. Markin, J. Therm. Anal. Calorim 98 (2009) 843–848.
[20] N. Chernorukov, A. Knyazev, N. Kuznetsova, A. Markin, N. Smirnova, Thermochim. Acta 470 (2008) 47.